

# Hole dominated transport in InGaAs metal semiconductor metal photodetectors

Marian Hargis and Stephen E. Ralph

*Department of Physics, Emory University, Atlanta, Georgia 30322*

Jerry Woodall and Dave McInturff

*Department of Electrical and Computer Engineering, Purdue University, West Lafayette, Indiana 47907-1285*

(Received 8 March 1995; accepted for publication 22 May 1995)

We report the direct measurement of the intrinsic photocurrent response of both top and back illuminated planar metal–semiconductor–metal structures. We directly observe the temporal dynamics of the hole transport dependence on applied bias and the initial spatial distribution using a near infrared tunable femtosecond light source and electrically biased structures. The increased hole transit time of back illuminated structures can be completely understood in terms of the hole velocity and the initial spatial distribution of the carriers. Additionally, we report the fastest directly measured 50  $\mu\text{m}$  diameter InGaAs photodetector with a 26 ps full width at half maximum. © 1995 American Institute of Physics.

InP-InGaAs based photodetectors operating in the fiber suitable wavelength regions of 1.3  $\mu\text{m}$  and 1.55  $\mu\text{m}$  are of the intense interest for high speed optical communication systems. The planar metal–semiconductor–metal (MSM) structure exhibits intrinsically lower capacitance per area than vertical PiN structures and has been shown to provide superior overall performance to the PiN structure.<sup>1</sup> Materials issues have previously hindered the MSM from achieving transit time performance levels and low dark currents. These difficulties include excessive residual carrier densities which precludes device depletion at low bias and the low Schottky barrier height of commonly used metals on InGaAs which permits excessive dark current. Larger contact barrier heights are achieved using wider bandgap Schottky enhancement layers.<sup>2</sup> Complete depletion of the absorbing layer at low bias is made possible by careful attention to growth conditions and the substrate buffer layer composition.<sup>3</sup>

Integration with optical fibers and the simultaneous elimination of the shadowing effects of the electrodes is achieved via back illumination. Although this has been associated with reduced bandwidth when compared to top illumination.<sup>4,5</sup> The details of the physical mechanisms causing this bandwidth reduction have never been reported.

Previous studies of the transport and performance of planar InGaAs structures have illustrated the importance of hole transport in these structures when illuminated through the top surface.<sup>6,7</sup> A thorough investigation of top illumination conditions has been given by Soole *et al.*<sup>8</sup> Additional work has also been reported on a variety of growth<sup>9</sup> and processing techniques.<sup>10</sup> In this letter we present the results of a detailed study of the bias voltage and wavelength dependence of InGaAs MSM structures for both top and bottom illumination conditions. We show that a proper consideration of carrier transport reveals that hole transit times dominate the long tail component of impulse response and are solely responsible for the differences between the top and bottom illumination photocurrent responses. We also show the interesting result that electrons experience fields which are above the peak velocity field and thus experience *increased* transit times for increasing bias greater than 5 V.

The structures consist of a 1.0  $\mu\text{m}$  thick  $\text{In}_{0.53}\text{Ga}_{0.47}\text{As}$  light absorbing layer followed by a graded Schottky enhancement layer. A 1000 Å AlInAs buffer layer was used at the Fe:InP substrate interface. The structures, each 50  $\mu\text{m}$  in diameter, were composed of interdigitated 1  $\mu\text{m}$  wide fingers and a gap ( $L_g$ ) between them of 2.0  $\mu\text{m}$ . The structures reported on here are transit time limited and together with a femtosecond light source allow the determination of intrinsic carrier transit times.

The near infrared femtosecond illumination pulses were obtained from an optical parametric oscillator (OPO) which produced  $\sim 150$  fs pulses tunable from 1.35  $\mu\text{m}$  to 1.6  $\mu\text{m}$ .<sup>11</sup> Accurate comparisons of the top vs substrate illumination responses were achieved utilizing a silicon wafer which had “V grooves” and reflectors etched in the top surface. Individual devices were positioned above these reflectors. The photocurrent was measured using a digital sampling scope with a bandwidth limited risetime of 17 ps. The measured pulse to pulse jitter was typically 600 fs.

Figure 1 depicts the normalized impulse response for both top and bottom illumination. The bottom (top) illumination case produced a typical responsivity of 0.8 A/W (0.35 A/W). The average power was 20  $\mu\text{W}$  (0.25 pJ/pulse) and the illumination wavelength was 1.36  $\mu\text{m}$ . The back illumination case shows a significantly enhanced long tail component. We have observed that the decay component is systematically larger for the back illumination case and that this is independent of illumination wavelength, bias, and illumination intensity. As a check of the carrier concentration dependence, we measured the photoresponse at 50  $\mu\text{W}$  and 20  $\mu\text{W}$  optical power. The observed photocurrents were nearly indistinguishable, establishing the absence of screening effects at these fluences. Thus, the changes observed in Fig. 1 cannot be attributed to the increased carrier number which occurs in the substrate illumination case due to the absence of obscuring electrodes. The measured pulse widths are similar, 26 ps top vs 29 ps bottom corresponding to a deconvolved full width at half maximum (FWHM) of 17 ps for top and 20 ps for bottom illumination. The directly observed FWHM represents the shortest reported for 50  $\mu\text{m}$  diameter

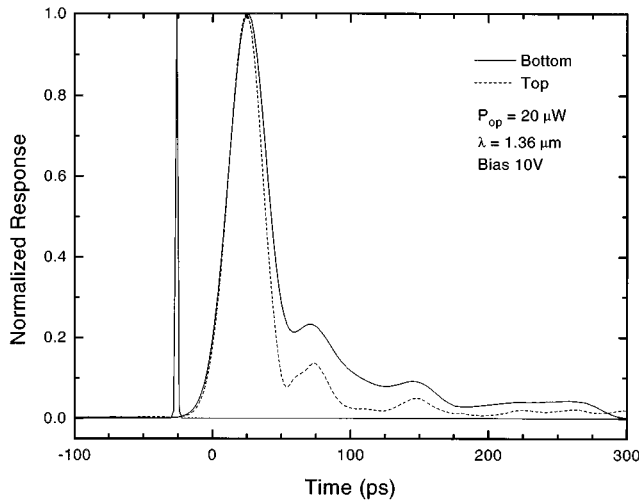


FIG. 1. The impulse response for top and bottom illumination of a 50  $\mu\text{m}$  diameter planar MSM structure biased at 10 V. The incident pulse width is depicted near  $t = -25$  ps.

$\text{In}_{0.53}\text{Ga}_{0.47}\text{As}$  MSM structures. These results are explained by observing that the electric field strength on the substrate side of the absorbing channel is always substantially less than the field strength on the electrode side of the channel. What is remarkable, however, is the degree to which the long decay component of the photoresponse is enhanced in the substrate illumination case *and* the nearly constant FWHM of the main peak.

We have used conformal mapping techniques to determine the potential and field profile throughout the alternating electrode structure.<sup>12</sup> These results are appropriate representations of the electric fields when the structure is fully depleted and the potential across the contact layers is negligible.<sup>13</sup> For the bias levels and low light intensities used these requirements are satisfied. The conformal mapping results show that the regions near the substrate interface have average field strengths less than 30 percent of the average field ( $V_{\text{applied}}/L_g$ ). We have found it useful to examine the velocity vs position profiles in the structure. Using the velocity-field relationships for InGaAs carriers<sup>14</sup> and the calculated field profiles we have determined the quasistatic carrier velocities in the structure. This neglects velocity overshoot and other transient effects which should be minimal for the times scales of interest. Figure 2(a) depicts the field lines and the average velocity for electrons in the planar structure for 5 V bias. In Fig. 2(b) the same field lines together with the quasistatic hole velocities are shown. Figure 2(a) depicts the interesting result that electrons which are furthest away from the electrodes actually possess a higher velocity. Although the electrical field strength falls off rapidly with increasing distance from the electrodes, the large negative differential velocity (NDV) of electrons in InGaAs results in this counter-intuitive behavior. The more conventional result for holes is shown in Fig. 2(b). The velocity smoothly decreases with increasing distance from the electrodes. The hole velocities near the substrate interface of  $1.4 \times 10^6$  cm/s are much less than the saturation velocity. At 10 V bias, the velocities of holes systematically increases while the ve-

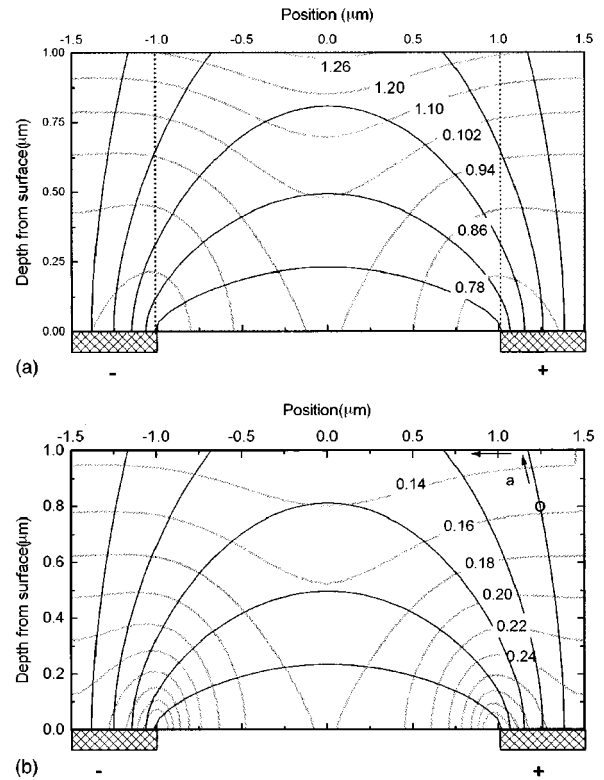


FIG. 2. (a) Quasi-steady-state electron velocity contours, shaded lines, for the MSM structure at 5 V bias. The contours are identified in units of  $10^7$  cm/s. The electric field lines (solid) are also included. (b) Hole velocity contours. Note the electron velocities increase with increasing distance from the electrodes.

locity of electrons decreases throughout most of the structure.

Unlike the top illumination case, back illumination generates a large density of carriers behind the electrodes (these regions are delineated by the dashed vertical lines in Fig. 2). Most of the carriers generated in this region which must be collected at the opposite contact, holes under the anode for instance, must first travel back toward the substrate and therefore encounter a large path length and a fraction encounter the buffer layer heterojunction [path *a* in Fig. 2(b)]. Only a small component of this small field moves the carriers along the hetero-interface, further reducing the velocity. The top illumination condition does not allow photogeneration in these regions and the fraction of photogenerated charge which encounters the back heterointerface is vastly smaller than that of the top illumination case.

We have calculated carrier transit times for various positions in the absorbing channel. Holes generated under the electrodes and near the substrate have a transit time of 253 ps [path *a* in Fig. 2(b)] to the opposite electrode. Electrons traveling a similar path have a transit time of 35 ps. In contrast, holes generated in the center of the structure have a transit time of 55 ps. We conclude (i) the majority of electrons are collected within 35 ps for both illumination conditions, (iii) substantial hole current continues for times greater than 200 ps for the back illumination case only.

In Fig. 3 the bias dependent photoresponse for 1.36  $\mu\text{m}$  excitation and 20  $\mu\text{W}$  average power is shown for both illu-

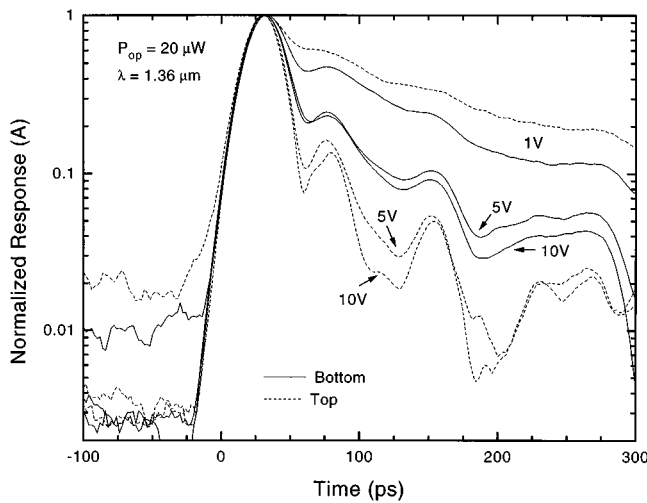


FIG. 3. The bias dependent photoresponse for  $1.36 \mu\text{m}$  excitation and  $20 \mu\text{W}$  average power for both top and bottom illumination conditions.

mination conditions. The features in the decay portion of the response result from inductance and impedance mismatch of the probe. For all biases observed, the back illumination has a larger slow component.

The results of Fig. 2 suggest that the long decay times of Fig. 3 are completely determined by hole transit times. Hole velocities throughout the structure should saturate at  $\sim 15 \text{ V}$  and the initial spatial distribution of carriers has a dramatic effect on average hole transit times. These are consistent with the observation that the largest bias measured of  $20 \text{ V}$  varied negligibly from the indicated  $10 \text{ V}$  response and was insufficient to produce a back illumination response commensurate with the  $5 \text{ V}$  top illumination case. Additionally, the back illumination case is expected to have significant hole current at times greater than  $200 \text{ ps}$  while the top illuminated structure should have substantially less hole current at these long delay times. Measurements performed at lower powers (carrier density  $< 10^{15} \text{ cm}^{-3}$ ) show the same long tail for the back illumination thus eliminating carrier pileup effects as the cause of the long tail.

Increasing bias is expected to produce only small changes in electron transit times. Indeed, electron transit times are expected to increase with increasing bias. The FWHM for top illumination changes from  $26 \text{ ps}$  to  $25 \text{ ps}$  for bias increases from  $5$  to  $15 \text{ V}$ . In contrast, we observe a slight increase with bias in the FWHM for the bottom illumination case, from  $27 \text{ ps}$  to  $31 \text{ ps}$  over the same bias range.

In Fig. 4 the photoresponse for two excitation wavelengths,  $1.36 \mu\text{m}$  and  $1.45 \mu\text{m}$  are shown for both illumination conditions at a bias of  $10 \text{ V}$ . Again, the data has been normalized to show the differences in the temporal characteristics. It is evident that the main peak, attributed to electrons, does not depend strongly on wavelength. However the long tail is sensitive illumination wavelength. The back illumination case shows an increased slow hole component for shorter wavelengths in contrast to the top illumination which shows a slight increase in slow hole component of longer wavelengths. These results are explained by absorption depth considerations. Using the measured absorption coefficients for our structures we can estimate the ratio of photogenerated

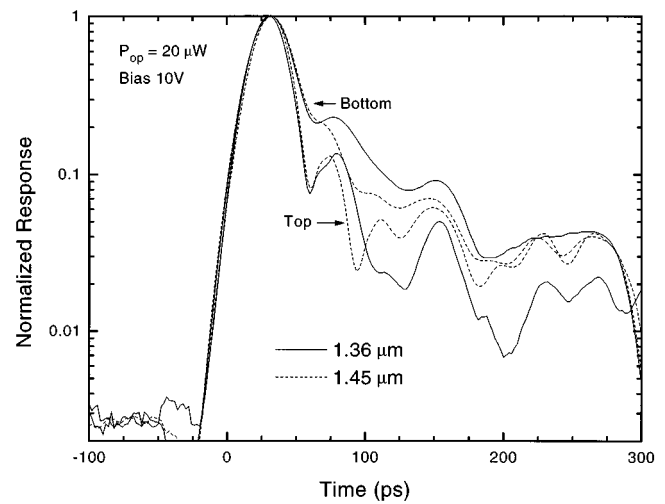


FIG. 4. The impulse response for  $1.36 \mu\text{m}$  and  $1.45 \mu\text{m}$ . Both top and bottom illumination conditions are shown.

carrier density at the substrate interface and the collection contact interface. For back illumination this ratio changes from  $3$  to  $1.36 \mu\text{m}$  to nearly  $2$  at  $1.45 \mu\text{m}$ . For back illumination, shorter wavelengths produce a higher concentration of carriers at the substrate interface, these remote carriers produce a longer tail as shown. The corresponding bandwidths for  $1.45 \mu\text{m}$  illumination are  $14.4 \text{ GHz}$  top and  $6.2 \text{ GHz}$  bottom illumination.

In conclusion we have measured the intrinsic photocurrent response of planar MSM structures and found a dramatically enhanced long tail component which we have attributed exclusively to increased average hole transit times. We also report increased electron transit times with increasing bias due to NDV.

This research was supported in part by the Georgia State Advanced Technology Development Center, and by GTE Laboratories Inc., Waltham MA. We also gratefully acknowledge the use of the Microelectronics Research Center at the Georgia Institute of Technology.

- <sup>1</sup>D. Rogers, *J. Lightwave Technol.* **9**, 1635 (1990).
- <sup>2</sup>D. Rogers, J. M. Woodall, G. D. Pettit, and D. McInturff, *IEEE Trans. Electron Devices* **ED-34**, 2383 (1987).
- <sup>3</sup>S. E. Ralph, M. C. Hargis, and G. D. Pettit, *Appl. Phys. Lett.* **61**, 2222 (1992).
- <sup>4</sup>P. Haugsjaa, G. A. Duchene, J. F. Mehr, A. J. Negri, and M. J. Tabasky, in *Proceedings of the IEEE LEOS Annual Meeting*, Boston, 1994 (IEEE, Piscataway, 1994), p. 61.
- <sup>5</sup>H. T. Griem, S. Ray, J. L. Freeman, and D. L. West, *Appl. Phys. Lett.* **56**, 1067 (1990).
- <sup>6</sup>J. B. D. Soole and H. Schumacher, *IEEE Trans. Electron Devices* **ED-37**, 2285 (1990).
- <sup>7</sup>S. Tiwari and M. A. Tischler, *Appl. Phys. Lett.* **60**, 1135 (1990).
- <sup>8</sup>J. B. D. Soole and H. Schumacher, *IEEE J. Quantum Electron.* **QE-27**, 737 (1991).
- <sup>9</sup>N. Debar, A. Rudra, J. Carlin, and M. Ilegems, *Appl. Phys. Lett.* **65**, 228 (1994).
- <sup>10</sup>U. Schade, St. Kollakowski, E. H. Botcher, and D. Bimberg, *Appl. Phys. Lett.* **64**, 1389 (1994).
- <sup>11</sup>We thank Spectra-Physics Lasers Inc. for the loan of the femtosecond optical parametric oscillator.
- <sup>12</sup>Y. C. Lim and R. A. Moore, *IEEE Trans. Electron Devices* **ED-15**, 173 (1968).
- <sup>13</sup>S. E. Ralph and D. Grishkowsky, *Appl. Phys. Lett.* **59**, 1972 (1991).
- <sup>14</sup>S. Adachi, *Physical properties of III-V semiconductor compounds* (Wiley, New York, 1992).